Earth and Planetary Science Letters 286 (2009) 41–51

Contents lists available at ScienceDirect

Earth and Planetary Science Letters

journal homepage: www.elsevier.com/locate/epsl

Rhenium–osmium isotopes and platinum-group elements in the Rum Layered Suite, Scotland: Implications for Cr-spinel seam formation and the composition of the Iceland mantle anomaly

Brian O'Driscoll [a,*], James M.D. Day [b], J. Stephen Daly [a], Richard J. Walker [b], William F. McDonough [b]

[a] UCD School of Geological Sciences, University College Dublin, Belfield, Dublin 4, Ireland
[b] Department of Geology, University of Maryland, College Park, MD 20742, United States

ARTICLE INFO

Article history:
Received 5 February 2009
Received in revised form 4 June 2009
Accepted 8 June 2009
Available online 25 July 2009

Editor: R.W. Carlson

Keywords:
Rum Layered Suite
Os isotopes
platinum-group elements
Cr-spinel seam formation
mantle
North Atlantic Igneous Province
Iceland

ABSTRACT

The Rum Layered Suite is a layered mafic–ultramafic body that was emplaced during Palaeogene North Atlantic margin rifting. It is a classic open-system magma chamber, constructed of 16 repeated coupled peridotite–troctolite units, some of which have laterally extensive ~2 mm-thick platinum-group element (PGE) enriched (~2 μg g^{-1}) Cr-spinel seams at their bases. In order to investigate Cr-spinel seam petrogenesis and enrichment of the PGE, abundances of these elements and Re–Os isotopes have been determined at three stratigraphic levels of the Rum Layered Suite that represent major magma replenishment events. Individual units preserve a range of initial $^{187}Os/^{188}Os$ ratios, demonstrating heterogeneity in the composition of replenishing magmas. Data for both the Cr-spinel seams and overlying silicates reveal that the processes that formed the Cr-spinel also concentrated the PGE, following magma replenishment. There is no evidence for structurally-bound PGE in Cr-spinel. Instead, the PGE budget of the Rum Layered Suite is linked to base metal sulphides, especially pentlandite, and to PGE alloys contained within the Cr-spinel seams, but which exist as separate phases at Cr-spinel grain boundaries. The range in initial Os isotope compositions ($\gamma_{Os} = 3.4$ to 36) in the Rum Layered Suite can be successfully modelled by 5–8% assimilation of Lewisian gneiss coupled with changing PGE contents in the replenishing magmas associated with sulphide removal. Initial $^{187}Os/^{188}Os$ ratios for Rum rocks range from 0.1305 to 0.1349 and are atypical of the convecting upper mantle, but are within the range for recently erupted picrites and basalts from Iceland and Palaeogene picrites and basalts from Baffin Island, Greenland and Scotland. Thus, the Os isotope data suggest that the North Atlantic Igneous Province magmas were collectively produced from a mantle source with components that remained relatively unchanged in Os isotopic composition over the past 60 Ma, and that likely contain a recycled lithospheric component.

1. Introduction

Large igneous provinces (LIPs) are the physical manifestation of short-timescale melting events, often associated with continental break-up (Ernst et al., 2005). The North Atlantic Igneous Province (NAIP) is one of the most intensely studied large igneous provinces (e.g., Saunders et al., 1997), and hosts a number of renowned layered intrusions, including the Rum Layered Suite, NW Scotland (Fig. 1), which was intruded at 60.53 ± 0.08 Ma (Hamilton et al., 1998), during Palaeogene opening of the North Atlantic. The Rum Layered Suite is widely regarded as a classic example of a layered mafic intrusion that formed by open-system magmatic differentiation (Brown, 1956; Wager and Brown, 1968; Emeleus et al., 1996), and early petrological studies of it contributed significantly to the development of the crystal settling and cumulus theory (Wager and Brown, 1968).

The relatively small size (15–18 km^3) of the Rum Layered Suite compared with the Bushveld, Stillwater or Muskox layered intrusions (>1000 km^3; Lambert et al., 1994; Eales and Cawthorn, 1996; Day et al., 2008) has helped to preserve primary stratigraphic variations in magmatic textural and geochemical features, which may be obscured in larger intrusions (Tepley and Davidson, 2003; Holness, 2005; O'Driscoll et al., 2007). Furthermore, addition of repeated magma pulses into the Rum magma chamber can, in some instances, be precisely monitored by the presence of Cr-spinel seams, allowing detailed study of the under- and overlying cumulates in the context of open-system magmatic processes. A controversial aspect of the Rum Cr-spinel seams and layered intrusion Cr-spinel seams in general is how and when they form. General models for Cr-spinel seam genesis typically involve open-system magma replenishment and hybridisation of compositionally distinct magmas (Irvine, 1975), but the mechanisms

* Corresponding author. School of Physical and Geographical Sciences, Keele University, Keele ST5 5BG, UK. Tel.: +44 1782 733184; fax: +44 1782 715261.
E-mail address: b.o'driscoll@esci.keele.ac.uk (B. O'Driscoll).

0012-821X/$ – see front matter © 2009 Elsevier B.V. All rights reserved.
doi:10.1016/j.epsl.2009.06.013

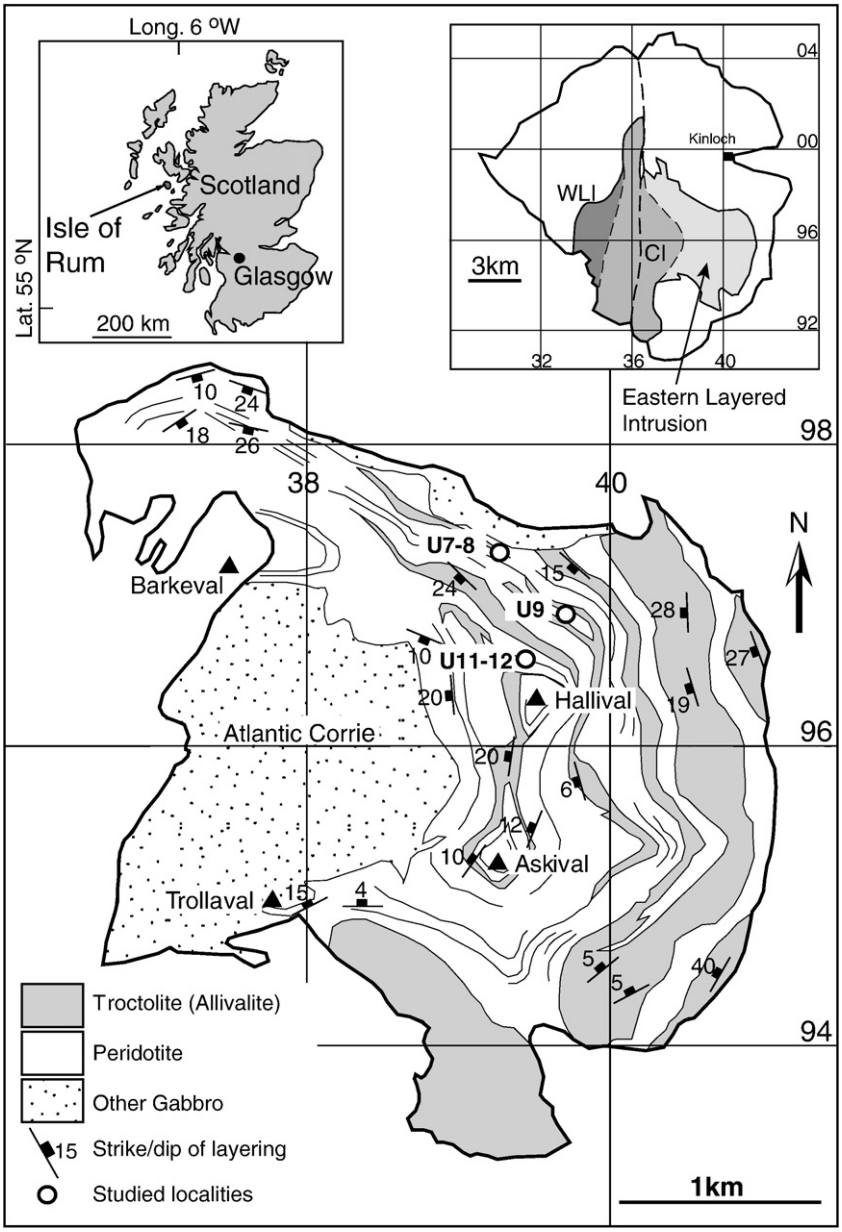

Fig. 1. Grid referenced map of the Rum Layered Suite with inset maps of the location of the Isle of Rum (top left) and major intrusive units on the island (top right). Top right inset map shows the location of the Eastern and Western Layered Intrusions and the Central Intrusion that make up the Rum Layered Suite. The geological map of the Eastern Layered Intrusion shows the sampling localities for the Unit 7–8, Unit 9 and Unit 11–12 sections studied here.

involved with, and timing of, Cr-spinel crystallization are debated (e.g., Spandler et al., 2005; Mondal and Mathez, 2007).

Platinum-group elements (PGE; Os, Ir, Ru, Rh, Pt, Pd – with Re and Au collectively termed highly siderophile elements – HSE) can provide insight into these processes, because they are intimately associated with Cr-spinel seams. The PGE and Re have both chalcophile and siderophile tendencies, with Os, Ir and Ru (IPGE; Barnes et al., 2008) being more compatible than Pt, Pd (PPGE) and Re, leading to a significant fractionation between these elements during igneous processes. Furthermore, the PGE include the ^{187}Re–^{187}Os system (half-life = ~42 Ga; Smoliar et al., 1996), which is useful in determining the sources of the PGE. Initial $^{187}Os/^{188}Os$ signatures have been used to infer that crustal contamination was important in generating the laterally extensive Cr-spinel seams in the Bushveld, Stillwater and Muskox layered intrusions, and that PGE enrichment is primarily a magmatic phenomenon (e.g., Lambert et al., 1989; Schoenberg et al., 1999; Horan et al., 2001; Day et al., 2008). It has also been proposed that initial Os isotope heterogeneity in the Bushveld intrusion may be inherited from an inhomogeneous mantle source (Richardson and Shirey, 2008), implying that similar mantle-derived variations may be present in other intrusions.

In this study, we focus on three stratigraphic levels in the Rum Layered Suite at which major magma replenishment events have been documented (Fig. 1). Petrological observations are coupled with Re–Os isotope and PGE and Re abundance data of different cumulate types at these discrete horizons, to address the formation of Cr-spinel seams. In addition, *in situ* analyses of sulphides and oxide phases are presented to quantify the mode of occurrence and mineral associations of the HSE within the seams, in order to understand enrichment processes in the Cr-spinel horizons (*c.f.* Barnes et al., 2006, 2008; Godel and Barnes, 2008). Finally, we demonstrate that inferences can be made regarding the Os isotope composition of the early stages of the NAIP, based on the Rum Layered Suite, and associated rocks.

2. Geological setting and sample details

This study focuses on the Eastern Layered Intrusion of the Rum Layered Suite (Fig. 1; Emeleus et al., 1996), which comprises 16 well-preserved, coupled feldspathic peridotite–troctolite (±olivine gabbro and anorthosite) cyclic units (Brown, 1956; Emeleus et al., 1996). Individual cyclic units of widely varying thickness comprise feldspathic peridotite overlain by troctolite and sometimes by clinopyroxene-rich olivine gabbro and/or anorthosite (Fig. 2). The basal peridotites are generally interpreted to represent fresh pulses of basalt and/or picritic magma (MgO = ~13.5 to 20.5 wt.%; Emeleus et al., 1996). Furthermore, cryptic variation in the cyclic units of the Eastern Layered Intrusion (Dunham and Wadsworth, 1978) implies complex fractionation after magma replenishment.

Rum peridotite olivine is compositionally similar to that of ultramafic layers in other large layered intrusions (e.g., Mg# = 84–86; Eales and Cawthorn, 1996) but has higher Ni (>1900 μg g^{-1}) than in the overlying troctolites (Mg# = 76–84; Ni ≤ 235 μg g^{-1}; Emeleus, 1997). Reversals in these trends occur immediately below the base of succeeding units, and are attributed to the local effects of chemical equilibration of minerals with overlying peridotite (Dunham and Wadsworth, 1978; Emeleus, 1997).

Cr-spinel seams (chromitite), at the junctions of some of the major cyclic units (e.g., 6–7, 7–8, 11–12 and 13–14) (Fig. 2), are usually 2–4 mm thick (Fig. 3a) and laterally extensive over several kilometres. The seams contain up to 60 vol.% Cr-spinel, and small (<0.1 mm) sulphide globules are common (Fig. 3b and c). Traditional models for Cr-spinel seam formation invoke settling of Cr-spinel crystals onto a pre-existing silicate mineral substrate, followed by olivine and plagioclase as the chromitite, peridotite and troctolite units crystallized (Fig. 2; Henderson and Suddaby, 1971; Dunham and Wilkinson, 1985). A new model for Rum Cr-spinel formation proposes assimilation

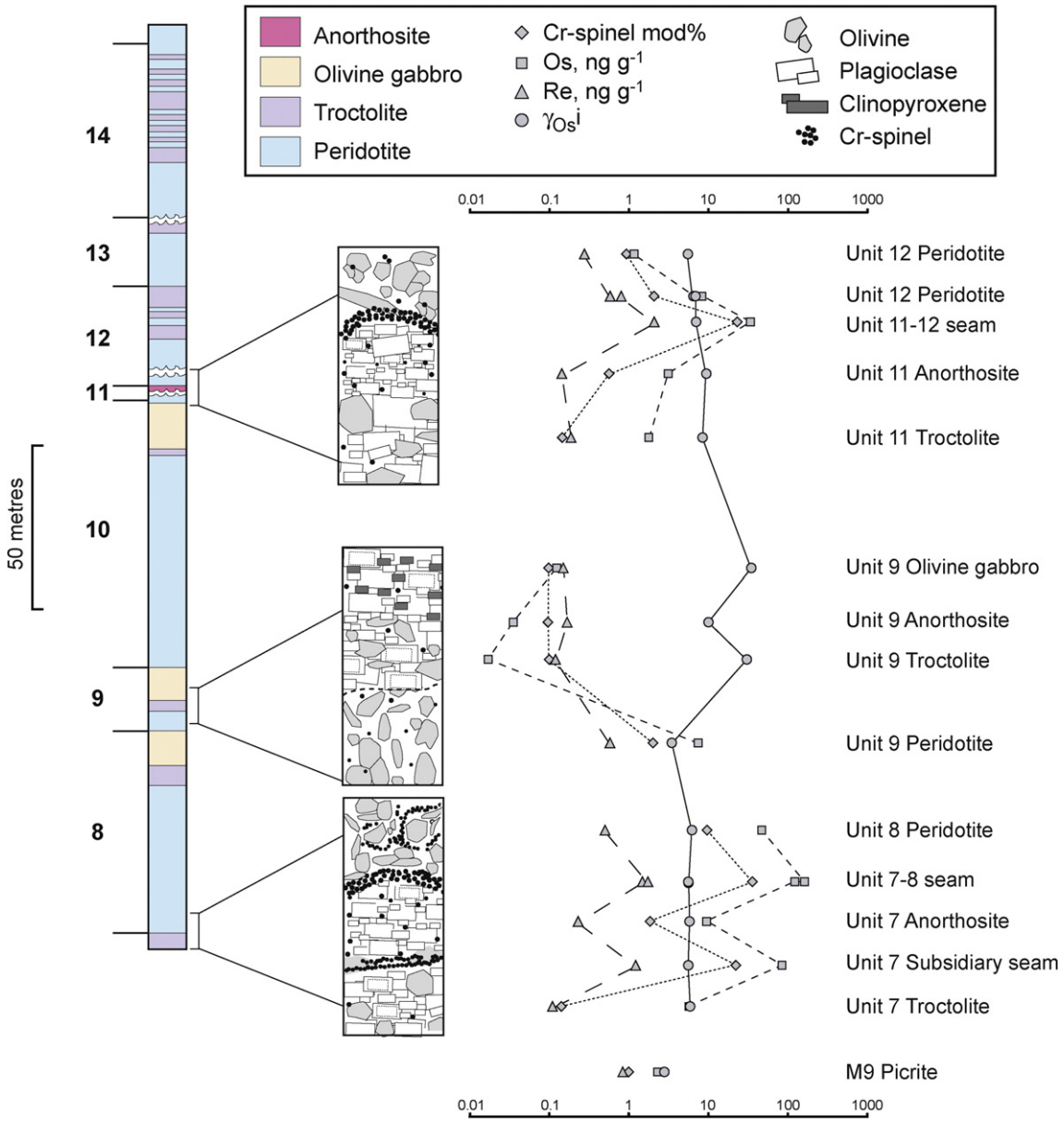

Fig. 2. Stratigraphic column of the cyclic Units 8 to 14 within the Eastern Layered Intrusion (adapted from Emeleus, 1997) and schematic diagrams of the textural relationships at unit boundaries. Stratigraphically controlled Re and Os abundance data (ng g^{-1}), Cr-spinel (modal %) and initial Os isotope composition (as γ_{Os}) are shown according to their relative positions within the illustrations of textures at the Unit 7–8, and Unit 11–12 boundaries and throughout Unit 9. Note the correlation between Os, Re and Cr-spinel modal abundances for all units.

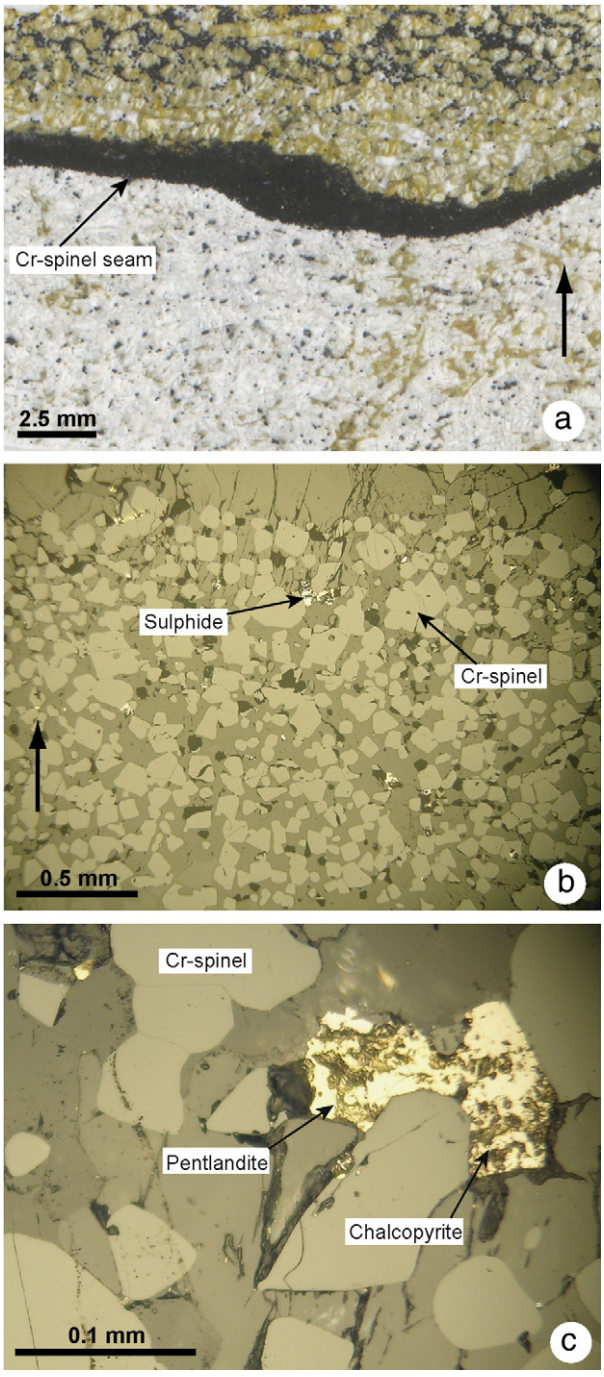

Fig. 3. (a) Thin section scan of the Unit 7–8 boundary, illustrating anorthosite overlain by a Cr-spinel seam that is capped by the Unit 8 peridotite (way-up arrowed). Note the high concentration of Cr-spinel in both the anorthosite and, approximately 0.5 cm above the seam in the peridotite. (b) Reflected light photomicrograph of the Unit 11–12 seam, showing the distribution of sulphide (highly reflective) amongst Cr-spinel crystals (way-up arrowed). (c) Reflected light images of the typical occurrence of a sulphide bleb, composed of pentlandite and chalcopyrite, in the Unit 7–8 Cr-spinel seam. Sulphides almost always occur at the edges of Cr-spinel crystals.

of cumulate troctolite by downward percolating picritic melt and *in situ* crystallization of the Cr-spinel seams within the crystal mush (O'Driscoll et al., 2009).

Chromitite, peridotite, troctolite and anorthosite were sampled astride the Unit 7–8 and 11–12 boundaries (Figs. 1 and 2), which have the best-developed and most laterally extensive Cr-spinel seams. Samples from Unit 9 (Fig. 2), which lacks a Cr-spinel seam associated with its peridotite, were analysed to investigate the behaviour of the PGE and Re in localities not associated with Cr-spinel seam formation. Unlike the Unit 8 and 12 peridotites, the Unit 9 peridotite has been shown to be intrusive into a plagioclase-rich crystal mush (Bédard et al., 1988; Holness, 2005). We also analysed a picritic dyke, believed to represent the parental liquid to Rum peridotites (M9; Emeleus et al., 1996; Upton et al., 2002). The picrite is crystal-rich and has a texture consistent with that of a partial cumulate. The generally fresh state of the samples (e.g., Fig. 3b and 3c) is confirmed by low loss on ignition values (0.1–1.7 wt.%; Table S1).

3. Analytical methods

Rhenium–osmium isotope and PGE analyses were performed at the University of Maryland. 0.1–0.13 g of chromitite and 0.8–0.9 g of other whole-rock powders were digested in sealed borosilicate Carius tubes using a 1:2 mix of 12 M HCl and 16 M HNO_3 at >260 °C for >36 h, with isotopically enriched multi-element spikes. We also performed a 48 h leaching experiment of the Unit 7–8 chromitite, using 1 M HF–HCl (150 °C), to examine the effect this had on PGE abundances in the sample and the likely location of these elements in mineral phases. Osmium was purified by solvent extraction and microdistillation, prior to measurement using a Triton thermal ionisation mass spectrometer in negative ion mode, where external analytical precision on $^{187}Os/^{188}Os$ ratios was better than 2‰ (2σ). Rhenium, Pd, Pt, Ru and Ir were purified using anion exchange separation techniques and were measured using an Element 2 ICP-MS. External analytical reproducibility (2σ) was better than 0.5% for Re, Ir and Pt and 1% for Pd and Ru. Blank corrections were generally negligible (<3% and typically ≪1%) for samples, with the exception of the Unit 9 troctolite, anorthosite and olivine gabbro, which have generally greater uncertainties resulting from blank correction (0.2–60%; average blank $^{187}Os/^{188}Os = 0.159 \pm 0.001$, 4 pg Re, 130 pg Pd, 24 pg Pt, 7 pg Ru, 4 pg Ir and 0.25 pg Os). The uncertainties relating to blank corrections do not affect petrogenetic interpretations made here. *In situ* laser-ablation ICP-MS analysis of sulphides was performed at the University of Maryland using a New Wave 213 nm laser-ablation system coupled to an Element 2 ICP-MS. Trace-element abundances were determined on individual spots, or in rasters, using a 12–55 μm-diameter laser diameter and a laser repetition rate of 7 Hz at 2–2.5 J/cm^2. Replicate LA-ICP-MS analyses of the University of Toronto JB sulphide yielded an external precision of 2% for all trace- and major-element compositions (2σ). Electron microprobe analyses of sulphides were performed at the University of Göttingen, Germany, and whole-rock major and trace element analyses were performed at the University of Leicester, UK. Further details of analytical methods are presented in the Supplementary materials section.

4. Results

4.1. Major- and minor-elements

Major- and minor-element compositions of anorthosites, troctolites, olivine gabbro, peridotite and the M9 picrite dyke demonstrate the control of plagioclase crystallization and accumulation in the intrusion, with strong negative correlations of plagiophile elements (e.g., Al, Ca, Sr) with Mg (Fig. S1 and Table S1, Supplementary materials). Peridotites are the most Mg-rich units in the Rum Layered Suite (36.2 to 37.2 wt.% MgO) and have high Ni and Cr contents (1830 to 2030 μg g^{-1} Ni, 2860 to 7060 μg g^{-1} Cr). The M9 picrite dyke is also MgO-, Ni- and Cr-rich (MgO = 34.3 wt.%), consistent with an origin as a partial cumulate.

4.2. Platinum-group element and Re abundances

Whole-rock PGE and Re abundance data for Rum are presented in Table 1 and in Fig. 4. PGE reproducibility on replicated samples is better than 5%, with the exception of Ir (28%) in the Unit 12 peridotite.

Table 1
Highly siderophile element and Os isotope data for the Rum Layered Suite, NW Scotland.

Sample	Unit	MgO (wt.%)	Os	Ir	Ru	Pt	Pd	Re	$^{187}Re/^{188}Os$	$\pm 2\sigma$	$^{187}Os/^{188}Os$	$\pm 2\sigma$	$^{187}Os/^{188}Os_i$	$\pm 2\sigma$	$\gamma_{Os}i$	$\pm 2\sigma$
Rum Layered Suite rocks																
Upper perid	11-12	37.2	1.160	0.766	2.372	1.010	8.038	0.277	1.17	0.018	0.13529	0.00014	0.1341	0.0003	5.5	0.2
Peridotite	11-12	36.2	8.369	4.830	10.57	104.7	201.9	0.592	0.344	0.005	0.13652	0.00005	0.1362	0.0001	7.1	0.1
Replicate			8.501	6.162	10.37	110.7	174.9	0.831	0.474	0.007	0.13717	0.00007	0.1367	0.0001	7.5	0.1
Chromitite	11–12	–	33.52	40.27	68.43	267.8	411.7	2.099	0.302	0.005	0.13702	0.00006	0.1367	0.0001	7.5	0.1
Anorthosite	11-12	0.7	3.211	3.178	2.988	32.27	8.879	0.151	0.232	0.003	0.13994	0.00008	0.1397	0.0002	9.9	0.1
Troctolite	11-12	22.3	1.861	1.738	1.714	9.99	7.518	0.199	0.525	0.008	0.13868	0.00010	0.1382	0.0002	8.6	0.2
Olivine gab	9	13.4	0.128	0.099	0.106	1.324	1.504	0.143	5.56	0.083	0.1780	0.0003	0.1726	0.0007	35.7	0.6
Anorthosite	9	10.3	0.0358	0.108	0.038	0.104	3.897	0.173	23.8	0.357	0.1635	0.0023	0.1401	0.0047	10.2	3.7
Troctolite	9	11.9	0.0178	0.003	0.054	0.146	0.478	0.124	34.4	0.516	0.1997	0.0010	0.1659	0.0024	30.4	1.9
Peridotite	9	36.5	7.423	3.323	7.140	14.82	6.895	0.579	0.378	0.006	0.13191	0.00006	0.1315	0.0001	3.4	0.1
Peridotite	7-8	–	47.16	35.81	66.45	121.6	32.43	0.488	0.0503	0.001	0.13497	0.00005	0.1349	0.0001	6.1	0.1
Chromitite	7-8	–	166.6	148.5	248.0	1872	1442	1.708	0.0495	0.001	0.13461	0.00006	0.1346	0.0001	5.8	0.1
Replicate			161.7	143.5	235.0	1854	1414	1.460	0.0436	0.001	0.13458	0.00007	0.1345	0.0001	5.8	0.1
Chromitite res.		–	124.6	108.1	161.3	1666	1465	1.724	0.0668	0.001	0.13452	0.00008	0.1345	0.0002	5.7	0.1
Anorthosite	7-8	3.7	9.468	7.534	14.35	80.59	67.54	0.226	0.117	0.002	0.13452	0.00006	0.1344	0.0001	5.7	0.1
Sub-chromitite	7-8	–	82.50	78.61	105.6	1200	963.3	1.174	0.0687	0.001	0.13422	0.00009	0.1342	0.0002	5.5	0.1
Troctolite	7-8	12.9	5.823	4.278	5.781	100.7	103.0	0.106	0.0910	0.001	0.13428	0.00007	0.1342	0.0001	5.5	0.1
Picrite dyke																
M9	Dyke	34.3	2.470	0.888	2.893	3.461	5.248	0.828	1.62	0.024	0.13210	0.00006	0.1305	0.0001	2.6	0.1

Abundance data for Os, Ir, Ru, Pt, Pd and Re are reported in ng g^{-1}. Initial $^{187}Os/^{188}Os$ ($^{187}Os/^{188}Os_i$) and $\gamma_{Os}i$ are calculated assuming an age of 60 Ma.

Reproducibility for Re ranges from 14 to 40%. A leached residue of the Unit 7–8 Cr-spinel seam displays consistently lower PGE and Re abundances than unleached sample fractions; an effect that is more pronounced for the IPGE than for the PPGE (Fig. 4c; Table 1). PGE abundances vary throughout the intrusion, and exhibit well-defined lithological and stratigraphic correlations (Fig. 2). Rhenium concentrations, however, are consistently low. Unit 7–8 and Unit 11–12 Cr-spinel seams show relative enrichments in Pt and Pd, with 'humpback-type' chondrite-normalized patterns (Fig. 4), similar to the neutron activation data of Power et al. (2000). Unit 7 and 11 troctolites and anorthosites have similar patterns, at lower overall abundances, to their respective Cr-spinel seams. Unit 11–12 rocks have higher Re/Os (0.05–0.24) and generally lower and more variable Pt/Ir (10.6 ± 7.8, 1σ) ratios than Unit 7–8 rocks (Re/Os = 0.01–0.02; Pt/Ir = 13.4 ± 4.4). The Unit 7–8 and Unit 11–12 PGE abundances are different from those of the Unit 9 rocks; the latter being relatively PGE-depleted. A chondrite-normalized pattern for the M9 picrite reveals an HSE pattern similar to ~60 Ma West Greenland picrites (Fig. 4).

4.3. Re–Os isotope systematics

Sub-chondritic Re/Os values for most samples means that measured and calculated initial $^{187}Os/^{188}Os$ are similar (Table 1). Only the upper peridotite sample from Unit 12, and olivine gabbro, anorthosite and troctolite samples from Unit 8–9 have supra-chondritic Re/Os. Of these, only the anorthosite and troctolite required substantial age corrections (>3%). Individual units preserve a range of initial $^{187}Os/^{188}Os$, with γ_{Os} values (percent deviation from a chondritic reference in initial $^{187}Os/^{188}Os$) ranging between +5.5 and +6.1 for Unit 7–8, +5.5 to +9.9 for Unit 11–12 and +3.4 to +35.7 for Unit 9. Duplicate dissolution and analysis of samples indicate reproducibility at a level better than ± 0.2 γ_{Os} units, so the variations apparently reflect real isotopic heterogeneity at the time of crystallization. The minimal isotopic variations in the lower unit (7–8) and greater isotopic variations in the higher units (9 and 11–12) reflect isotopic heterogeneity within the evolving magma. The highest γ_{Os} values were obtained from the Unit 9 anorthosite, troctolite and olivine gabbro, at an intermediate level in the stratigraphy (Fig. 2; Table 1). These observations contrast with the Stillwater Complex, where γ_{Os} values and Os isotopic heterogeneity decrease up stratigraphy (Horan et al., 2001). As a consequence of isotopic heterogeneity, the collective Rum Layered Suite data do not define an isochron (Fig. 5). Similar Os isotope heterogeneity has also been observed in larger and far older intrusions (e.g., Lambert et al., 1989; Day et al., 2008). Although Unit 9 exhibits the largest $^{187}Re/^{188}Os$–$^{187}Os/^{188}Os$ variations, these data, from a single unit, do not define an isochron. This indicates that, even at the scale of individual units, there were significant variations in initial $^{187}Os/^{188}Os$. The Unit 9 peridotite and M9 picrite have the lowest γ_{Os} values (+3.4 and +2.6, respectively; Fig. 5). Our ^{187}Re–^{187}Os data (Table 1) for the M9 picrite dyke are in close agreement with previous analysis of a similar dyke rock reported by Upton et al. (2002).

4.4. Sulphide mineral compositions

Sulphide grains in the Unit 7–8 and Unit 11–12 Cr-spinel seams are small (typically <100 μm), compared with those in other intrusions (typically >1000 μm; e.g., Barnes et al., 2008; Godel and Barnes, 2008). The sulphides usually comprise ≤1 vol.% of the seam, and occur at the edges and interstices of Cr-spinel crystals (Fig. 3b and c). HSE abundance data for sulphides from both seams are characterized by higher concentrations of Os, Ir, Ru, Rh and Pd compared with Pt, Re and Au (Table 2 and Table S2, Supplementary materials) with up to 2 μg g^{-1} total PGE abundances present in the seams. Sulphides in the Unit 11–12 Cr-spinel seam are predominantly pentlandite with lesser proportions of chalcopyrite and pyrrhotite, as well as chalcocite and bornite. The Unit 7–8 Cr-spinel seam is dominated by sub-equal quantities of chalcopyrite and pyrrhotite with minor pentlandite. A number of non-stoichiometric phases, that we interpret to represent monosulphide solid solution, were also measured.

5. Discussion

5.1. Siting of the PGE within the Rum Layered Suite

An important question relating to the PGE and Re in mafic–ultramafic intrusions is their host mineral locations, particularly within Cr-spinel seams (e.g., Godel and Barnes, 2008). It is possible to group whole-rock PGE behaviour on plots of Ir relative to Os, Ru, Pt, Pd and Re (Fig. 6). These plots help to establish an order of compatibility for the Rum Layered Suite that is identical to that reported for the Muskox Intrusion (Day et al., 2008):

$$D_{Ir} \sim D_{Os(0.995)} \sim D_{Ru(0.993)} > D_{Pt(0.965)} > D_{Pd(0.941)} > D_{Re(0.602)}.$$

The numbers shown in parentheses denote correlation coefficients (R^2) for the HSE slopes relative to Ir and are a general estimation of compatibility, incorporating variations in bulk partition coefficients. Positive correlations are revealed between the PGE and other compatible elements (e.g., MgO, Cr, Ni; Supplementary Tables S1 and S3), establishing a link with major mineral phases, such as olivine and Cr-spinel (Fig. 2).

In most lithologies, the PGE are hosted within sulphide minerals, or as metal alloys (e.g., Ballhaus et al., 2006), rather than in oxide or silicate minerals. In detailed studies of platinum-group minerals (PGM) in Rum Cr-spinel seams, Butcher et al. (1999) and Power et al. (2000) identified native Pt, alloys (Pd–Cu, Pt–Fe), laurite, sperrylite, moncheite, isomertiete, cooperite and braggite along with a variety of less common arsenide, bismuthide, telluride and sulphide minerals, with most grains being smaller than 6 μm. They also found that over 70% of PGM were associated with sulphides (50% in pentlandite, 25% in chalcopyrite) and only 1% with Cr-spinel (Power et al., 2000).

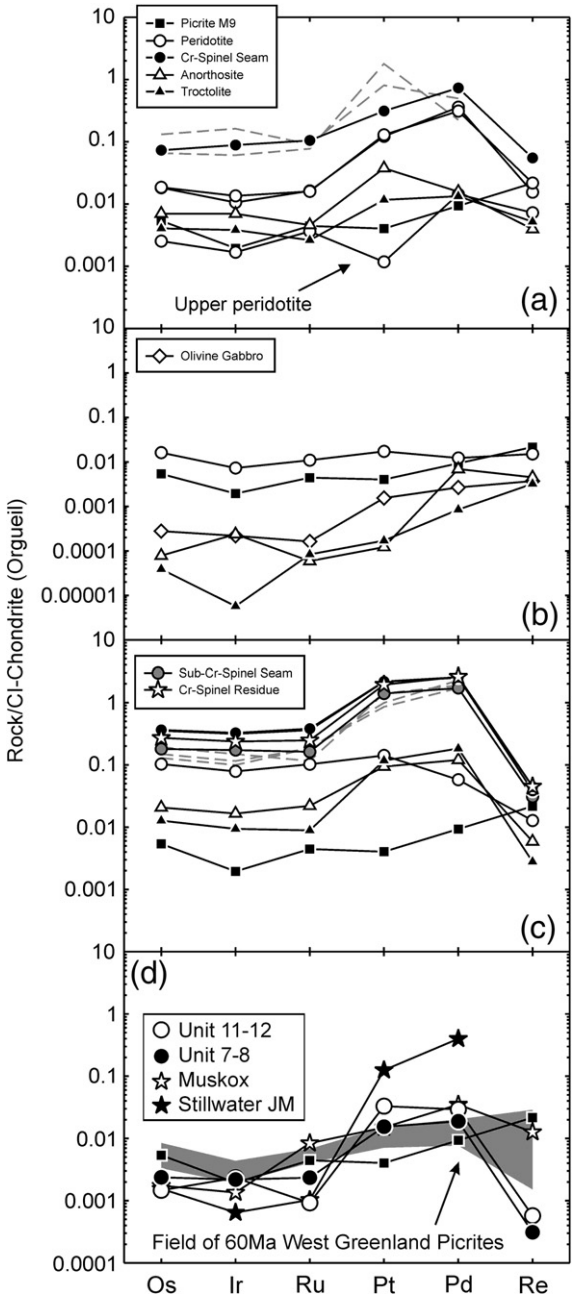

Fig. 4. CI-chondrite-normalized (Orgueil; Horan et al., 2003) highly siderophile element patterns for Rum Layered Suite rocks from (a) Unit 11–12, (b) Unit 9 and (c) Unit 7–8. (d) Estimated parental melt compositions for peridotites, gabbros, troctolites and anorthosites (Unit 7–12) and the Unit 7–8 Cr-Spinel Seam (Unit 7–8; *N*-factor = 45,000, $D^{Sul/Sil}$ = 20,000) are compared with estimated parental melts from the Muskox Intrusion (Day et al., 2008), Stillwater J-M Reef (Godel and Barnes, 2008) and the field of data for 60 Ma West Greenland Picrites (Woodland, 1999) — see text for details. The picrite sample, M9, is shown in all panels for comparative purposes. Whole-rock neutron activation analysis data for Unit 11–12 and Unit 7–8 from Power et al. (2000) are shown as dashed-grey lines in (a) and (c).

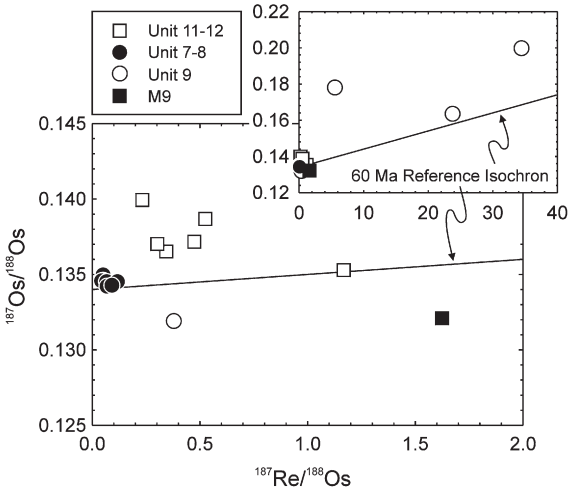

Fig. 5. $^{187}Re/^{187}Os$–$^{187}Os/^{188}Os$ plot of Rum Layered Suite rocks. Inset shows the full range of measured $^{187}Re/^{187}Os$–$^{187}Os/^{188}Os$ measured in Unit 9. We interpret the non-isochronous relations of the units to reflect isotopic heterogeneity in replenishing magmas. Also shown is a 60 Ma reference isochron with an initial $^{187}Os/^{188}Os$ ratio of 0.134.

The typically small size of PGM grains (~1–2 μm) compared with the laser-beam diameter used for analysis (12–55 μm) means that the HSE compositions for Rum sulphide minerals likely represent amalgamations of host sulphide minerals and PGM. Indeed, micro-nuggets enriched in the HSE were encountered on a number of occasions during time-resolved laser-ablation analysis of Unit 7–8 and Unit 11–12 sulphides, especially close to grain boundaries (Figs. S2 and S3, Supplementary materials). These observations, in natural samples, support experimental evidence for concentration of PGM minerals at grain boundaries (Finnigan et al., 2008). The lack of PGM inclusions in Cr-spinel is confirmed by multiple raster analyses of Cr-spinels from the Unit 7–8 and Unit 11–12 seams, which show no appreciable concentrations of the HSE.

Thus, base metal sulphide minerals (pentlandite, pyrrhotite, chalcopyrite) and associated PGM (discrete Pt- and Os–Ir–Ru alloys and as bismuthides, tellurides, arsenides and sulphides) likely control the HSE budget in Rum Cr-spinel seams (Fig. 6). The distribution of HSE in sulphide within Unit 7–8 and Unit 11–12 Cr-spinel seams is comparable to that found by Godel and Barnes (2008) for PGE in the platiniferous J-M Reef of the Stillwater Complex. They noted that Pd was the dominant PGE (>95%) in J-M Reef sulphides, with Pt being restricted to PGM and not sulphide phases. Palladium (>45%) is the dominant HSE in Unit 7–8 and Unit 11–12 Cr-spinel seam sulphides, although Pd is less abundant than in J-M reef sulphides, and is mainly hosted in pentlandite. We also found that Pt was normally hosted as discrete phases, implying that Pt is located in PGM rather than within sulphide. Leaching of the Unit 7–8 Cr-Spinel seam resulted in a 25% reduction in Os and Ir, 35% reduction in Ru and a 10% reduction in Pt concentrations with no observed changes in Pd or Re compared with the unleached sample digestions. This experiment was designed to remove silicate as well as HCl-soluble phases, so we interpret fractionation of Os, Ir and Ru from Pt, Pd and Re to imply that the PPGE and IPGE are associated with different phases (sulphides and PGM alloys), consistent with the LA-ICP-MS analysis of sulphides and

Table 2
Average sulphide compositions in the Eastern Layered Intrusion, Rum Layered Series Unit 11–12 and 7–8 Cr-spinel seams.

	(wt.%)						(μg g^{-1})							
Phase	S	Cu	Ni	Se	Fe	Co	Os	Ir	Ru	Rh	Pt	Pd	Re	Au
Unit 11–12														
Pyrrhotite	36.2	0.21	0.66	0.04	62.9	0.02	3.0	8.4	12.7	8.3	1.1	20.6	0.3	5.3
Pentlandite	35.4	32.9	0.13	0.04	32.4	0.02	10.7	22.6	34.2	20.7	61.1	366	0.9	5.6
Chalcopyrite	33.6	0.73	28.6	0.07	37.3	0.51	4.8	6.7	18.8	6.1	1.7	96.4	<1.1	6.2
MSS	34.9	19.3	11.1	0.04	35.6	0.14	4.3	29.9	30.0	41.5	1.1	806	<0.3	n.m.
Unit 7–8														
Pyrrhotite	36.7	0.13	0.20	0.05	64.8	0.01	10.6	20.5	22.9	13.8	24.1	62.5	0.4	1.1
Pentlandite	34.9	32.1	1.66	0.03	32.1	0.08	5.9	5.5	10.8	3.0	2305	141	0.9	<0.3
Chalcopyrite	34.0	1.57	25.6	0.06	39.2	0.47	<0.5	0.1	<15.0	3.8	0.6	32.8	<1.5	0.2
MSS	36.9	4.18	3.49	0.06	55.9	0.07	3.4	184	21.9	16.1	49.2	65.7	<0.4	<0.8

MSS: Monosulphide solution.

associated minerals. These results are also consistent with the observation of Schoenberg et al. (1999), that sulphide minerals of Bushveld Cr-spinel seams are enriched in the PGE compared to Cr-spinel.

In Fig. 6, we show calculations of the quantity of sulphide within Rum Layered Suite rocks, assuming all HSE are hosted within sulphide and associated PGM, and that the average composition of chalcopyrite, pyrrhotite and pentlandite corresponds to those found in the Unit 7–8 Cr-spinel seam. The models imply that 1% sulphide is present in the Unit 7–8 Cr-spinel seam, with lesser proportions for the Unit 11–12 seam. Less than 0.001% of the Unit 7–8 sulphide is required to explain the HSE within the lowest HSE abundance troctolites and anorthosites. The amount of sulphide calculated for the Unit 7–8 and Unit 11–12 Cr-spinel seams is consistent with the modal abundance of sulphide in these samples and confirms the control of HSE abundances by sulphides in the Rum Layered Suite. We also estimate the abundance of HSE in the parental melt of Rum Layered Suite rocks using the extrapolation method employed by Day et al. (2008), which compares HSE in troctolites, anorthosites, gabbros and peridotites with compatible element abundances, and the zone refining method of Brügmann et al. (1993) using Cr-spinel HSE abundances. Both methods dominantly reflect the parental melt composition of the unit with the highest Os contents (Unit 7–8) and yield parental melt compositions that are in close agreement (0.7–1 ng g^{-1} Os, 0.7–1.1 ng g^{-1} Ir, 0.6–1.5 ng g^{-1} Ru, 13.4–28.5 ng g^{-1} Pt, 10.7–16.6 ng g^{-1} Pd and 0.012–0.023 ng g^{-1} Re). Further, the estimated IPGE concentrations are similar to those reported for the Muskox Intrusion (Day et al., 2008) and Stillwater (Godel and Barnes, 2008) parental melts (Fig. 4), and are similar to NAIP picrites (Dale et al., 2009).

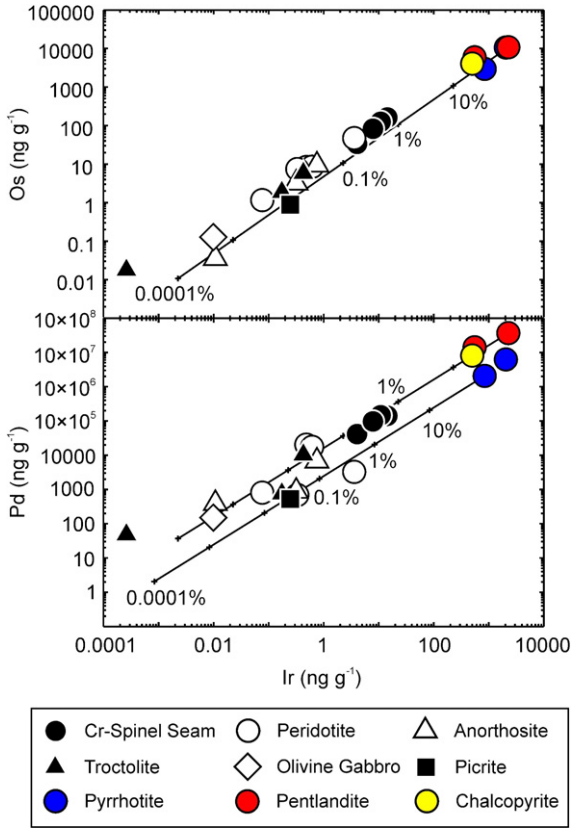

Fig. 6. Plots of Os and Pd versus Ir in the Rum Layered Suite, with average compositions of major sulphide phases (pentlandite, chalcopyrite and pyrrhotite) from the Unit 7–8 and Unit 11–12 Cr-spinel seams as measured by LA-ICP-MS (Table 2; Figure S4). Rum Layered Suite HSE data are consistent with strong sulphide control and with S-saturation during Cr-spinel formation, with progressively S- and PGE-poor magmas forming increasingly more Mg- and Cr-poor units. Models show calculated quantities of sulphide in percent increments by mass for pentlandite and pyrrhotite and illustrate that ~1% sulphide (dominantly pentlandite) is required to explain the HSE abundances observed in the Cr-spinel seams, consistent with observed modal abundance variations.

5.2. Open-system magma chamber dynamics and Os isotope heterogeneity

The relatively young age and restricted size of the Rum Layered Suite are advantageous for understanding Re–Os isotope and PGE behaviour during magmatic differentiation because: 1) they enable evaluation of initial isotopic heterogeneity within the intrusion and: 2) despite evidence for high-temperature sub-solidus interaction with meteoric waters from oxygen isotope ratios (Greenwood et al., 1992), there is no evidence for significant post-magmatic re-equilibration (e.g., Tepley and Davidson, 2003), or serpentinisation, which can cause open-system behaviour of Re in the magmatic pile (Day et al., 2008). Additionally, clear stratigraphic control on Cr-spinel seams and sulphides in the Rum Layered Suite is not consistent with a hydrothermal origin for PGE enrichment (Power et al., 2000).

Evidence for open-system behaviour in the Rum Layered Suite comes from clear magma replenishment episodes at unit boundaries and cryptic compositional variations marked by more fayalitic olivine or less anorthitic plagioclase up stratigraphy (Emeleus, 1997). Cryptic variation in Unit 10 has been attributed to progressive fractionation in cooling magma batches, with compositional reversals at unit tops, reflecting infiltration of fresh primitive magma into underlying cumulates (Dunham and Wadsworth, 1978). Open-system behaviour also occurred in Unit 14, where thin subsidiary peridotites alternate with troctolite (Renner and Palacz, 1987). Osmium isotopic heterogeneity in the Rum Layered Suite supports the open-system magma chamber model. Isotopic shifts within the units (γ_{Os} +5.5 to +6.1 and +5.5 to +9.9 for Unit 7–8 and Unit 11–12, respectively) indicate changes in both the chemical and isotopic compositions of the magma as replenishment events and crystallization of units proceeded.

In addition to complex open-system magma chamber replenishment events, there is evidence for crust assimilation in the Rum Layered Suite. Strontium isotopic heterogeneity occurs at the crystal scale in Unit 9 troctolites and olivine gabbros, reflecting the growth of crystals in melts that underwent variable contamination by country rocks (Tepley and Davidson, 2003). Strontium, Pb and Nd isotope studies of the Eastern Layered Intrusion (Palacz, 1984, 1985; Palacz and Tait 1985) have concluded that magmas forming the troctolites experienced up to 7% crustal contamination of Lewisian amphibolite-facies gneiss, but that crustal contamination of basaltic and picritic parental melts to the basal peridotites was limited (Palacz, 1985; Palacz and Tait, 1985; Meyer et al., 2009). There is also evidence for primitive melt compositions in the Rum samples. It has previously been demonstrated that the M9 dyke, which has the lowest γ_{Os} of Rum rocks measured in this study (+2.6), reflects a primitive mantle melt based on Sr–Nd–Pb isotopic and trace element arguments (Upton et al., 2002; Meyer et al., 2009). We therefore use the Nd and Os isotope composition of this dyke as an endmember to model crustal assimilation in the Rum Layered Suite (Fig. 7). Because the M9 picrite dyke is a partial cumulate we do not use the Os content of this sample in the model, but instead initially estimate this parameter to be ~1 ng g^{-1} Os using zone refining and extrapolation methods (Section 5.1).

Despite heterogeneous distribution of PGE and Re in the continental crust (e.g., Peucker-Ehrenbrink and Jahn, 2001), it is possible to estimate the composition of crustal assimilants to Rum Layered Suite magmas from prior studies of Os and Nd isotopes in locally-derived crustal rocks. Lewisian mafic–ultramafic crust has elevated $^{187}Os/^{188}Os$ (0.170 to 1412, age corrected to 60 Ma) and low to moderate Os abundances (30 to 850 pg g^{-1}), but associated quartzofeldspathic gneiss and metasediments, which are considered the most likely Rum contaminants (Palacz, 1985; Meyer et al., 2009) are generally characterized by low Os abundances (<50 pg g^{-1}) and elevated $^{187}Os/^{188}Os$ (up to 5.7 with an average of ~2.36 at 60 Ma; Burton et al., 2000; Dale et al., 2009). We use the Nd isotope compositions and abundance of local quartzofeldspathic Lewisian gneiss from Meyer et al. (2009) and the 'average' Os crustal composition from Dale et al. (2009) for the crustal endmember in Fig. 7.

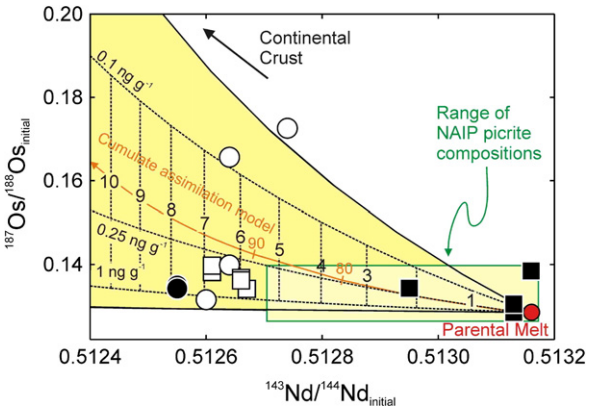

Fig. 7. Tracking crustal contamination and cumulate assimilation in the Rum Layered Suite using initial $^{187}Os/^{188}Os$ versus $^{143}Nd/^{144}Nd$ (60 Ma). We assume mixing between a parental melt ($^{187}Os/^{188}Os = 0.1285$; $^{143}Nd/^{144}Nd = 0.51316$; Nd = 8 μg g^{-1}; see text for details) of variable Os content (1 to 0.1 ng g^{-1}, see Fig. 6), versus a 'best estimate' continental crust value ($^{187}Os/^{188}Os = 2.36$; Os = 0.031 ng g^{-1}; $^{143}Nd/^{144}Nd = 0.51135$; Nd = 48 μg g^{-1}; Dale et al., 2009; Meyer et al., 2009) in percent (%) increments. The shaded field is the estimated limit of assimilation by variable Os abundance, $^{187}Os/^{188}Os$ composition continental crust (see Fig. 4 of Dale et al., 2009). Also shown is a cumulate assimilation model assuming an Nd composition for the cumulate assimilant of the Unit 10 gabbro (1.4 μg g^{-1} Nd, −2.3 ε_{Nd}; Palacz, 1985) and an Os composition of the Unit 9 troctolite (Table 1). Nd isotope data for Rum rocks can be found in Supplementary Table S4 and the field of NAIP picrites compositions is adapted from Dale et al. (2009). Symbols used are the same as those in Fig. 5.

An important aspect of modelling crustal assimilation in cumulate rocks is that they do not represent liquids but are crystals that precipitated from magmas, so the abundance of compatible elements like the PGE will be dominantly controlled by mineral/melt partition coefficients, with isotopic compositions reflecting the magmas they crystallized from. Therefore, in order to model the range in Os and Nd isotope compositions, the Os contents of the parental melts to individual cumulate rocks become an important parameter. For example, Os being scavenged from the melt during the generation of peridotites and Cr-spinel seams will lead to the formation of troctolites, anorthosites and gabbros from parental melts with lower Os contents, in turn leading to greater sensitivity of $^{187}Os/^{188}Os$ to *in situ* crustal contamination. Modelling parental melts assuming a range in Os contents from 1 ng g^{-1} to 0.1 ng g^{-1} can account for the entire range of Os isotope variations within the Rum Layered Suite via 5 to 8% crustal assimilation in parental melts (Fig. 7). Therefore, cumulate layers derived from parental melts with elevated Os abundances (1 ng g^{-1}) are less sensitive to the effects of crustal contamination than parental melts with lower Os abundances (<1 ng g^{-1}). From this observation we recognise that the M9 picrite dyke, the Unit 9 peridotite and the Unit 7–8 rocks have been least affected by crustal assimilation and thus record the best estimate of the Rum parental melt composition ($^{187}Os/^{188}Os = 0.1305$ to 0.1349, $\gamma_{Os} = +2.6$ to +6.1).

5.3. Os isotope constraints on Cr-spinel formation in the Rum Layered Suite

Cr-spinel seams in some of the world's largest layered intrusions exhibit considerable Os isotopic heterogeneity that exceeds the Os isotopic variations for the present-day convecting upper mantle. For example, the 2.06 Ga Bushveld ($\gamma_{Os} = +10$ to +55; Schoenberg et al., 1999), 2.70 Ga Stillwater ($\gamma_{Os} = +12$ to +34; Lambert et al., 1994; Horan et al., 2001) and 1.27 Ga Muskox intrusion ($\gamma_{Os} = +12.7$ to +25.2; Day et al., 2008) all exhibit elevated γ_{Os}, attributed to assimilation and mixing of crustally-contaminated melts with mantle-derived magmas. Layered intrusions with lower γ_{Os} such as the 2.58 Ga Great Dyke ($\gamma_{Os} = -6.9$ to +4.4; Schoenberg et al., 2003) and the 2.04 Ga Ipueira–Medrado sill ($\gamma_{Os} = -4.6$ to +3.3; Marques et al., 2003) are also considered to have significant crustal input, although in the case of these intrusions there may be a component from depleted continental lithosphere, which drives the composition of the magmas to sub-chondritic Os isotope compositions. Hence, in many PGE-mineralised stratiform Cr-spinel seam occurrences there appears to be an important role for magma mixing and contamination by continental crust (Day et al., 2008).

The range in γ_{Os} for the Rum Cr-spinel seams ($\gamma_{Os} = +5.5$ to +7.5) precludes a significant involvement of continental lithospheric mantle, as was concluded from studies employing trace elements and Sr–Nd–Pb isotopes (e.g., Palacz, 1985; Palacz and Tait, 1985). Instead, it has been proposed that the Rum Cr-spinel seams formed via assimilation of low-Si troctolitic cumulate within the pre-existing cumulate pile (Huppert and Sparks, 1980; Renner and Palacz, 1987; O'Driscoll et al., 2009). Two features of the Rum Cr-spinel seams are important in this regard. First, the Unit 7–8 Cr-spinel seam has less radiogenic γ_{Os} and a higher Os abundance than the later Unit 11–12 Cr-spinel. Second, γ_{Os} shows little variation across each of the Unit 7–8 and 11–12 boundaries, whether the rock type is anorthosite, troctolite, chromitite or peridotite; a feature that is qualitatively consistent with a melt-infiltration and cumulate assimilation model. Combined with the observation that Cr-spinel abundance correlates with Os concentration (Fig. 2), there appears to be a strong link between magma replenishment and Cr-spinel crystallization. In Fig. 7 we model the effect of cumulate assimilation on the composition of a

parental melt entering the Rum magma chamber. This model can explain the difference in γ_{Os} between Unit 7–8 and 11–12 through assimilation of underlying troctolites that have been variably crustally contaminated, and would reflect increasing contamination up stratigraphy, in marked contrast to the Stillwater Igneous Complex (Horan et al., 2001). A cumulate assimilation model can successfully account for both Os and Nd isotopes if >90% of the Os in the Unit 11–12 Cr-spinel seam derives from locally re-melted troctolite assuming the most radiogenic Os and unradiogenic Nd for this unit. Such a model provides permissible evidence for this process acting locally to melt up to 60% of the underlying troctolite cumulate (O'Driscoll et al., 2009).

An alternative explanation for the difference in γ_{Os} between the Unit 7–8 and 11–12 Cr-spinel seams is that they were generated from magmas with different initial Os contents. On average, the lithologies of Unit 7–8 are enriched by a factor of 4 relative to Unit 11–12, consistent with derivation from a melt more enriched in the PGE, and this can similarly explain the difference in γ_{Os} between the two units (Fig. 7). Given the limited evidence for S-saturation of magmas prior to entry into the Rum magma chamber and the similar Mg-number of the Unit 7–8 and 11–12 peridotites, this could imply lower degree partial melts feeding the later units. Based on experimental data for sulphide solubility in mafic magmas (Mavrogenes and O'Neill, 1999), it is unlikely that the possible differences in parental magma PGE contents relate to S-saturation prior to emplacement into the Rum magma chamber (Upton et al., 2002). Thus, sulphides in the Cr-spinel seams likely formed in the Rum magma chamber at or near the time of seam formation. This may have occurred in one of two ways: 1) through hybridisation of the new magma as a result of assimilation of cumulate mush (*c.f.* Irvine, 1975), or; 2) through immiscible sulphide liquid separation at the edges of Cr-spinel crystals that were undergoing a peritectic reaction with interstitial melt in the crystal mush, explaining the limited volumes of sulphide observed (O'Driscoll et al., 2009). Sulphide control and PGM alloy formational constraints from the Rum Layered Suite are of particular interest in *R*-factor models for PPGE enrichment in other layered intrusions (e.g., the Stillwater Complex; Campbell et al., 1983), where the separation of small volumes of sulphide is crucial.

5.4. The mantle source of Rum and the NAIP

Present-day Iceland volcanism can be traced back to magmatic events beginning at ~63 Ma, during the opening of the North Atlantic, which formed the British Palaeogene Igneous Province (BPIP) and NAIP (Saunders et al., 1997; Chambers et al., 2005). High Os abundance Rum Layered Suite rocks and associated picritic dykes, which represent the best estimates of Rum parental magmas, have γ_{Os} (+2.6) in the range measured for modern-day Icelandic picrites and basalts (γ_{Os} = 0 to +9; Skovgaard et al., 2001; Brandon et al., 2007). Furthermore, the Nd isotope compositions of the least contaminated Rum magmas (picrite dykes) overlap with those of Icelandic lavas (ε_{Nd} = +6 to +10; Upton et al., 2002). The calculated IPGE parental melt compositions for Rum are similar to the M9 picrite as well as high-MgO tholeiites from Iceland (Momme et al., 2003) and Hawai'i (Bennett et al., 2000) and Os abundances of NAIP picrites (Dale et al., 2009), implying that Rum parental magmas were generated from an S-undersaturated source (Fig. 4). These results indicate that the mantle sources feeding Rum and Iceland magmatism were broadly similar, in terms of Os and Nd isotopes, and that the Rum magmas resulted from relatively high degrees of partial melting (>15%; Mavrogenes and O'Neill, 1999), similar, to slightly less than that implied for picritic magmas in West Greenland and Baffin Island at ~60 Ma (Herzberg and O'Hara, 2002).

High Os abundance Rum lithologies also have γ_{Os} values that also overlap with, or are less radiogenic than, 'plume-derived', younger, high Os (>0.4 ng g^{-1}) Skye Main Lava Series (SMLS; γ_{Os} = +4.6 to +13) and Mull Plateau Group lavas (MPG; γ_{Os} = +3.0 to +23.5; Schaefer et al., 2002), 61.3 to 60.9 Ma high MgO, high Os (>0.4 ng g^{-1}) Ma West Greenland picrites (γ_{Os} = ~0 to +7.5; Schaefer et al., 2000; Dale et al., 2009), 56 to 54 Ma East Greenland (γ_{Os} = −1 to +2; Brooks et al., 1999; Peate et al., 2003), and ~61 Ma Baffin Island picrites (γ_{Os} = −0.3 to +5.6; Dale et al., 2009). Although some of these rocks have experienced assimilation of ancient, Os-poor crust characterized by radiogenic $^{187}Os/^{188}Os$, others are considered to reflect mantle compositions (e.g., Schaefer et al., 2000; Dale et al., 2009) and the overlap in compositions is remarkable given the likely heterogeneous nature of lithosphere through which their parental magmas traversed. Lavas in the NAIP with distinct Os isotopic compositions formed during the later stages of magmatism by melting of a depleted MORB mantle reservoir (Preshal Mhor group of Skye; γ_{Os} = −5; Schaefer et al., 2002), or from a significant interaction with continental lithospheric mantle (Manîtdlat Member of the Vaigat Formation, West Greenland; γ_{Os} = −16; Larsen et al., 2003) and clearly differ from Rum Layered Suite compositions.

One model to explain the high-MgO magmas in the early phases of NAIP magmatism invokes anomalous, hot mantle upwelling in response to, or as the cause of, incipient rifting of the North Atlantic. The 'mantle plume' model, while contentious, is supported by high $^{3}He/^{4}He$ signatures in 60 Ma picrites and modern Icelandic lavas (e.g., Stuart et al., 2003; Brandon et al., 2007). Independent evidence of moderately radiogenic $^{187}Os/^{188}Os$, low initial $^{18}O/^{16}O$ values (with respect to MORB) and uniform $^{186}Os/^{188}Os$ of Icelandic lavas suggests that the mantle source beneath Iceland contains at least one recycled component, as well as depleted MORB mantle and a relatively undepleted reservoir to account for high $^{3}He/^{4}He$ ratios (Skovgaard et al., 2001; Macpherson et al., 2005; Thirlwall et al., 2006; Brandon et al., 2007). A study of the SMLS and related rocks has revealed that the BPIP is characterized by elevated $^{3}He/^{4}He$ (Stuart et al., 2003). The Rum Layered Suite formed early in the history of the NAIP (Hamilton et al., 1998; Chambers et al., 2005) and preserves Os and Nd isotopic compositions that overlap with present-day Icelandic magmas, and to the Ordlingassoq member picrites of West Greenland. It is also clear that younger, high-MgO magmatism in the BPIP (SMLS and MPG lavas) and in Greenland also preserve radiogenic initial $^{187}Os/^{188}Os$ relative to MORB. These lines of evidence point to identical mantle source components in the NAIP over 60 Ma, with respect to Os, and provide possible evidence for recycled lithospheric components in magmas feeding the Rum Layered Suite as also suggested for other NAIP lavas (Schaefer et al., 2002; Brandon et al., 2007; Dale et al., 2009).

6. Conclusions

Variations in initial $^{187}Os/^{188}Os$ in different units of the Rum Layered Suite are interpreted to reflect magmatic heterogeneity, and support the classic open-system model for its emplacement. Cr-spinel seams mark the levels at which magma replenishment occurred and have similar initial $^{187}Os/^{188}Os$ ratios to the associated mafic and ultramafic cumulates above and below. Osmium and PGE abundance data also correlate with Cr-spinel modal abundance in all rock-types. This suggests that Os concentration is intrinsically linked to Cr-spinel crystallization, and thus, points to a primary magmatic origin for the seams. LA-ICP-MS analyses reveal that PGE abundances of up to ~2 μg g^{-1} in the seams are hosted primarily in interstitial sulphides, particularly pentlandite. Cr-spinel does not host any of the PGE. The majority of the Rum rocks have Os concentrations and initial $^{187}Os/^{188}Os$ ratios within the range for modern day picrites and basalts on Iceland, purportedly the modern day expression of the mantle anomaly responsible for the opening of the North Atlantic. This suggests that the melted products of this mantle source have changed little over ~60 Ma and may reflect the presence of recycled lithosphere in the Rum mantle source.

Acknowledgements

We are grateful to Graeme Nicoll for the M9 picrite sample, Tom Culligan for excellent thin-sections, Andreas Kronz for technical assistance on the Göttingen University electron microprobe and Richard Ash for assistance with LA-ICP-MS analysis. O'Driscoll acknowledges an IRCSET Postdoctoral Fellowship at University College Dublin and support from the University College Dublin Seed Funding Scheme. WFM gratefully acknowledges support from NSF grant #0739006. We are grateful to R.M. Ellam and an anonymous reviewer for their helpful comments and R.W. Carlson for his editorial assistance.

Appendix A. Supplementary data

Supplementary data associated with this article can be found, in the online version, at doi:10.1016/j.epsl.2009.06.013.

References

Ballhaus, C., Bockrath, C., Wohlgemuth-Ueberwasser, C., Vera Laurenz, V., Berndt, J., 2006. Fractionation of the noble metals by physical processes. Contrib. Mineral. Petrol. 152, 667–684.

Barnes, S.-J., Cox, R.A., Zientek, M.L., 2006. Platinum-group element, gold, silver and base metal distribution in compositionally zoned sulphide droplets from the Medvezky Creek mine, Noril'sk, Russia. Contrib. Mineral. Petrol. 152, 187–200.

Barnes, S.-J., Prichard, H.M., Cox, R.A., Fisher, P.C., Godel, B., 2008. The location of the chalcophile and siderophile elements in platinum-group element ore deposits (a textural, microbeam and whole rock geochemical study): implications for the formation of the deposits. Chem. Geol. 248, 295–317.

Bédard, J.H., Sparks, R.S.J., Renner, R., Cheadle, M.J., Hallworth, M.A., 1988. Peridotite sills and metasomatic gabbros in the Eastern Layered Series of the Rhum Complex. J. Geol. Soc. Lond. 145, 207–224.

Bennett, V.C., Norman, M.D., Garcia, M.O., 2000. Rhenium and platinum group element abundances correlated with mantle source components in Hawaiian picrites: sulphides in the plume. Earth Planet. Sci. Lett. 183, 513–526.

Brandon, A.D., Graham, D.W., Waight, T., Gautason, B., 2007. ^{186}Os and ^{187}Os enrichments and high-^{3}He/^{4}He sources in the Earth's mantle: evidence from Icelandic picrites. Geochim. Cosmochim. Acta 71, 4570–4591.

Brooks, C.K., Keays, R.R., Lambert, D.D., Frick, L.R., Nielsen, T.F.D., 1999. Re–Os isotope geochemistry of Tertiary picritic and basaltic magmatism of East Greenland: constraints on plume–lithosphere interactions and the genesis of the Platinova reef, Skaergaard Intrusion. Lithos 47, 107–126.

Brown, G.M., 1956. The layered ultrabasic rocks of Rhum, Inner Hebrides. Philos. Trans. R. Soc. B 240, 1–53.

Brügmann, G.E., Naldrett, A.J., Asif, M., Lightfoot, P.C., Gorbachev, N.S., Fedorenko, V.A., 1993. Siderophile and chalcophile metals as tracers of the evolution of the Siberian Trap in the Noril'sk region, Russia. Geochim. Cosmochim. Acta 57, 2001–2018.

Burton, K.W., Capmas, F., Birck, J.-L., Allègre, C.J., Cohen, A.S., 2000. Resolving crystallisation ages of Archean mafic-ultramafic rocks using the Re–Os isotope system. Earth Planet. Sci. Lett. 179, 453–467.

Butcher, A.R., Pirrie, D., Prichard, H.M., Fisher, P., 1999. Platinum-group mineralization in the Rum layered intrusion, Scottish Hebrides, UK. J. Geol. Soc. Lond. 156, 213–216.

Campbell, I.H., Naldrett, A.J., Barnes, S.J., 1983. A model for the origin of the platinum-rich sulphide horizons in the Bushveld and Stillwater Complexes. J. Petrol. 24, 133–165.

Chambers, L.M., Pringle, M.S., Parrish, R.R., 2005. Rapid formation of the Small Isles Tertiary centre constrained by precise ^{40}Ar/^{39}Ar and U–Pb ages. Lithos 79, 367–384.

Dale, C.W., Pearson, D.G., Starkey, N.A., Stuart, F.M., Ellam, R.M., Larsen, L.M., Fitton, J.G., Macpherson, C.G., 2009. Osmium isotopes in Baffin Island and West Greenland picrites: implications for the ^{187}Os/^{188}Os composition of the convecting mantle and the nature of high ^{3}He/^{4}He mantle. Earth Planet. Sci. Lett. 278, 267–277.

Day, J.M.D., Pearson, D.G., Hulbert, L.J., 2008. Rhenium–osmium isotope and platinum-group element constraints on the origin and evolution of the 1.27 Ga Muskox layered intrusion. J. Petrol. 49, 1255–1295.

Dunham, A.C., Wadsworth, W.J., 1978. Cryptic variation in the Rhum layered intrusion. Mineral. Mag. 42, 347–356.

Dunham, A.C., Wilkinson, F.C.F., 1985. Sulphide droplets and the Unit 11/12 chromespinel band, Rhum: a mineralogical study. Geol. Mag. 122, 539–548.

Eales, H.V., Cawthorn, R.G., 1996. The Bushveld Complex. In: Cawthorn, R.G. (Ed.), Layered Intrusions. Elsevier, Amsterdam, pp. 181–230.

Emeleus, C.H., 1997. Geology of Rum and the adjacent islands. Memoir of the British Geological Survey, Sheet 60 (Scotland).

Emeleus, C.H., Cheadle, M.J., Hunter, R.H., Upton, B.G.J., Wadsworth, W.J., 1996. The Rum Layered Suite. In: Cawthorn, R.G. (Ed.), Layered igneous rocks. Elsevier, Amsterdam, pp. 403–440.

Ernst, R.E., Buchan, K.L., Campbell, I.H., 2005. Frontiers in large igneous province research. Lithos 79, 271–297.

Finnigan, C.S., Brenan, J.M., Mungall, J.E., McDonough, W.F., 2008. Experiments and models bearing on the role of chromite as a collector of platinum group minerals by local reduction. J. Petrol. 49, 1647–1665.

Godel, B., Barnes, S.-J., 2008. Platinum-group elements in sulfide minerals and the whole rocks of the J-M Reef (Stillwater Complex): implication for the formation of the reef. Chem. Geol. 248, 272–294.

Greenwood, R.C., Fallick, A.E., Donaldson, C.H., 1992. Oxygen isotope evidence for major fluid flow along the contact zone of the Rum ultrabasic intrusion. Geol. Mag. 129, 243–246.

Hamilton, M.A., Pearson, D.G., Thompson, R.N., Kelley, S.P., Emeleus, C.H., 1998. Rapid eruption of Skye lavas inferred from precise U–Pb and Ar–Ar dating of the Rum and Cuillin plutonic complexes. Nature 394, 260–263.

Henderson, P., Suddaby, P., 1971. The nature and origin of chrome-spinel of the Rhum layered intrusion. Contrib. Mineral. Petrol. 33, 21–31.

Herzberg, C., O'Hara, M.J., 2002. Plume-associated ultramafic magmas of Phanerozoic age. J. Petrol. 43, 1857–1883.

Holness, M.B., 2005. Spatial constraints on magma chamber replenishment events from textural observations of cumulates: the Rum Layered Intrusion, Scotland. J. Petrol. 46, 1585–1600.

Horan, M.F., Morgan, J.W., Walker, R.J., Cooper, R.W., 2001. Re–Os isotopic constraints on magma mixing in the peridotite zone of the Stillwater complex, Montana, USA. Contrib. Mineral. Petrol. 141, 446–457.

Horan, M.F., Walker, R.J., Morgan, J.W., Grossman, J.N., Rubin, A.E., 2003. Highly siderophile elements in chondrites. Chem. Geol. 196, 27–42.

Huppert, H.E., Sparks, R.S.J., 1980. The fluid dynamics of a basaltic magma chamber replenished by influx of hot, dense ultrabasic magma. Contrib. Mineral. Petrol. 75, 279–289.

Irvine, T.N., 1975. Crystallisation sequences in the Muskox intrusion and other layered intrusions—II. Origin of chromitite layers and other similar deposits of other magmatic ores. Geochim. Cosmochim. Acta 39, 991–1020.

Lambert, D.D., Morgan, J.W., Walker, R.J., Shirey, S.B., Carlson, R.W., Zientek, M.L., Koski, M.S., 1989. Rhenium–osmium and samarium–neodymium isotopic studies of the Stillwater Complex. Science 244, 1169–1174.

Lambert, D.D., Walker, R.J., Morgan, J.W., Shirey, S.B., Carlson, R.W., Zientek, M.L., Lipin, B.R., Koski, M.S., Cooper, R.L., 1994. Re–Os and Sm–Nd isotope geochemistry of the Stillwater Complex, Montana: implications for the petrogenesis of the J-M Reef. J. Petrol. 35, 1717–1753.

Larsen, L.M., Pedersen, A.K., Sundvoll, B., Frei, R., 2003. Alkali picrites formed by melting of old metasomatised lithospheric mantle: Manîtdlat member, Vaigat formation, Palaeocene of West Greenland. J. Petrol. 44, 3–38.

Macpherson, C.G., Hilton, D.R., Day, J.M.D., Lowry, D., Grönvold, K., 2005. High-^{3}He/^{4}He depleted mantle and low-δ^{18}O recycled oceanic lithosphere in the source of central Icelandic lavas. Earth Planet. Sci. Lett. 233, 411–427.

Marques, J.C., Ferreira Filho, C.F., Carlson, R.W., Pimentel, M.M., 2003. Re–Os and Sm–Nd isotope and trace element constraints on the origin of the chromite deposit of the Ipueira-Medrado sill, Bahia, Brazil. J. Petrol. 44, 659–678.

Mavrogenes, J.A., O'Neill, H.S.C., 1999. The relative effects of pressure, temperature and oxygen fugacity on the solubility of sulfide in mafic magmas. Geochim. Cosmochim. Acta 63, 1173–1180.

Meyer, R., Nicoll, G.R., Hertogen, J., Troll, V.R., Ellam, R.M., Emeleus, C.H., 2009. Trace element and isotope constraints on crustal anatexis by upwelling mantle melts in the North Atlantic Igneous Province: an example from the Isle of Rum, NW Scotland. Geol. Mag. 146, 382–399.

Momme, P., Óskarsson, N., Keays, R.R., 2003. Platinum-group elements in the Icelandic rift system: melting processes and mantle sources beneath Iceland. Chem. Geol. 196, 209–234.

Mondal, S.K., Mathez, E.A., 2007. Origin of the UG2 chromitite layer, Bushveld Complex. J. Petrol. 48, 495–510.

O'Driscoll, B., Hargraves, R.B., Emeleus, C.H., Troll, V.R., Donaldson, C.H., Reavy, R.J., 2007. Magmatic lineations inferred from anisotropy of magnetic susceptibility fabrics in Units 8, 9, and 10 of the Rum Eastern Layered Series, Scotland. Lithos 98, 27–44.

O'Driscoll, B., Donaldson, C.H., Daly, J.S., Emeleus, C.H., 2009. The roles of melt infiltration and cumulate assimilation in the formation of a Cr-spinel seam in the Rum Eastern Layered Intrusion, NW Scotland. Lithos 111, 6–20.

Palacz, Z.A., 1984. Isotopic and geochemical evidence for the evolution of a cyclic unit in the Rhum intrusion, north-west Scotland. Nature 307, 618–620.

Palacz, Z.A., 1985. Sr–Nd–Pb isotopic evidence for crustal contamination in the Rhum intrusion. Earth Planet. Sci. Lett. 74, 35–44.

Palacz, Z.A., Tait, S.R., 1985. Isotopic and geochemical investigations of cyclic unit 10 from the Eastern Layered Series of the Rhum intrusion, north west Scotland. Geol. Mag. 122, 485–490.

Peate, D.W., Baker, J.A., Blichert-Toft, J., Hilton, D.R., Storey, M., Kent, A.J.R., Brooks, C.K., Hansen, H., Pedersen, A.K., Duncan, R.A., 2003. The Prinsen af Wales Bjerge formation lavas, East Greenland: the transition from tholeiitic to alkalic magmatism during Palaeogene continental break-up. J. Petrol. 44, 279–304.

Peucker-Ehrenbrink, N., Jahn, B.M., 2001. Rhenium–osmium isotope systematics and platinum-group element concentrations: loess and the upper continental crust. Geochem. Geophys. Geosyst. 2 art. no.-2001GC000172.

Power, M.R., Pirrie, D., Anderson, J.C.O., Butcher, A.R., 2000. Stratigraphical distribution of platinum-group minerals in the Eastern Layered Series, Rum, Scotland. Miner. Depos. 35, 762–775.

Renner, R., Palacz, Z.A., 1987. Basaltic replenishment of the Rhum magma chamber: evidence from Unit 14. J. Geol. Soc. Lond. 144, 961–970.

Richardson, S.H., Shirey, S.B., 2008. Continental mantle signature of Bushveld magmas and coeval diamonds. Nature 453, 910–913.

Saunders, A.D., Fitton, J.G., Kerr, A.C., Norry, M.J., Kent, R.W., 1997. The North Atlantic Igneous Province (in large igneous provinces: continental, oceanic, and planetary flood volcanism). Geophys. Monogr. 100, 45–93.

Schaefer, B.F., Parkinson, I.J., Hawkesworth, C.J., 2000. Deep mantle plume osmium isotope signature from west Greenland Tertiary picrites. Earth Planet. Sci. Lett. 175, 105–118.

Schaefer, B.F., Parkinson, I.J., Hole, M.J., Kerr, A.C., Scarrow, J.H., Rogers, N.W., 2002. Re–Os isotope systematics of the British Tertiary Volcanic Province: multiple mantle sources in the proto-Iceland plume. Geochim. Cosmochim. Acta 66, A672 (Supplement).

Schoenberg, R., Kruger, F.J., Nagler, T.F., Meisel, T., Kramers, J.D., 1999. PGE enrichment in chromitite layers and the Merensky Reef of the Bushveld complex; a Re–Os and Rb–Sr isotope study. Earth Planet. Sci. Lett. 172, 49–64.

Schoenberg, R., Naegler, T.F., Gnos, E., Kramers, J.D., Kamber, B.S., 2003. The source of the Great Dyke, Zimbabwe, and its tectonic significance; evidence from Re–Os isotopes. J. Geol. 111, 565–578.

Skovgaard, A.C., Storey, M., Baker, J., Blusztajn, J., Hart, S.R., 2001. Osmium–oxygen isotope evidence for a recycled and strongly depleted component in the Icelandic mantle plume. Earth Planet. Sci. Lett. 194, 259–275.

Smoliar, M.I., Walker, R.J., Morgan, J.W., 1996. Re–Os ages of group IIA, IIIA, IVA and IVB iron meteorites. Science 271, 1099–1102.

Spandler, C., Mavrogenes, J., Arculus, R., 2005. Origin of chromitites in layered intrusions: evidence from chromite-hosted melt inclusions from the Stillwater Complex. Geology 33, 893–896.

Stuart, F.M., Lass-Evans, S., Fitton, J.G., Ellam, R.M., 2003. High $^{3}He/^{4}He$ ratios in picritic basalts from Baffin Island and the role of a mixed reservoir in mantle plumes. Nature 423, 57–59.

Tepley, F.J., Davidson, J.P., 2003. Mineral-scale Sr-isotope constraints on magma evolution and chamber dynamics in the Rum layered intrusion, Scotland. Contrib. Mineral. Petrol. 145, 628–641.

Thirlwall, M.F., Gee, M.A.M., Lowry, D., Mattey, D.P., Murton, B.J., Taylor, R.N., 2006. Low $\delta^{18}O$ in the Icelandic mantle and its origins: evidence from the Reykjanes ridge and Icelandic lavas. Geochim. Cosmochim. Acta 70, 993–1019.

Wager, L.R., Brown, G.M., 1968. Layered Igneous Rocks. Oliver and Boyd, Edinburgh. 588 pp.

Woodland, S.J., 1999. Development of ICP-MS isotope dilution preconcentration techniques for determination of platinum group elements in volcanic rocks. Unpublished PhD thesis, The University of Durham. 384pp.

Upton, B.G.J., Skovgaard, A.C., McClurg, J., Kirstein, L., Cheadle, M., Emeleus, C.H., Wadsworth, W.J., Fallick, A.E., 2002. Picritic magmas and the Rum ultramafic complex, Scotland. Geol. Mag. 139, 437–452.